

***SYNCHROTRON STUDY OF METAL LOCALIZATION  
IN TYPHA LATIFOLIA L. ROOT SECTIONS***

Qian, Y., Feng, H., Gallagher, F. J., Zhu, Q., Wu, M., Liu, C.-J., Jones, K. W.,  
and Tappero, R. V.

Accepted for publication in  
*Journal of Synchrotron Radiation*

September 2015

**Environmental & Climate Sciences Dept.**

**Brookhaven National Laboratory**

**U.S. Department of Energy  
DOE Office of Science**

Notice: This manuscript has been authored by employees of Brookhaven Science Associates, LLC under Contract No. DE-SC0012704 with the U.S. Department of Energy. The publisher by accepting the manuscript for publication acknowledges that the United States Government retains a non-exclusive, paid-up, irrevocable, world-wide license to publish or reproduce the published form of this manuscript, or allow others to do so, for United States Government purposes.

This preprint is intended for publication in a journal or proceedings. Since changes may be made before publication, it may not be cited or reproduced without the author's permission.

## **DISCLAIMER**

This report was prepared as an account of work sponsored by an agency of the United States Government. Neither the United States Government nor any agency thereof, nor any of their employees, nor any of their contractors, subcontractors, or their employees, makes any warranty, express or implied, or assumes any legal liability or responsibility for the accuracy, completeness, or any third party's use or the results of such use of any information, apparatus, product, or process disclosed, or represents that its use would not infringe privately owned rights. Reference herein to any specific commercial product, process, or service by trade name, trademark, manufacturer, or otherwise, does not necessarily constitute or imply its endorsement, recommendation, or favoring by the United States Government or any agency thereof or its contractors or subcontractors. The views and opinions of authors expressed herein do not necessarily state or reflect those of the United States Government or any agency thereof.

1           **Synchrotron Study of Metal Localization in *Typha latifolia* L. Root Sections**

2   Yu Qian<sup>1#</sup>, Huan Feng<sup>1\*</sup>, Frank J. Gallagher<sup>2</sup>, Qingzhi Zhu<sup>3</sup>, Meiyin Wu<sup>4</sup>, Chang-Jun  
3   Liu<sup>5</sup>, Keith W. Jones<sup>6</sup>, Ryan V. Tappero<sup>6</sup>,

4   1. Department of Earth and Environmental Studies, Montclair State University, Montclair,  
5   New Jersey 07043, USA

6   2. Environmental Planning and Design Program, Department of Landscape Architecture,  
7   Rutgers, The State University of New Jersey, New Brunswick, New Jersey 08901, USA

8   3. School of Marine and Atmospheric Science, State University of New York, Stony  
9   Brook, NY 11794, USA

10   4. Department of Biology and Molecular Biology, Montclair State University, Montclair,  
11   New Jersey 07043, USA

12   5. Biosciences Department, Brookhaven National Laboratory, Upton, New York 11973,  
13   USA

14   6. Photon Sciences Directorate, Brookhaven National Laboratory, Upton, New York  
15   11973, USA

16   # Current Address: School of Ecology and Environmental Sciences, Yunnan University,  
17   Kunming, Yunnan, 650091 China

1 **Abstract**

2 Understanding mechanisms that control plant root metal assimilation in soil is critical to  
3 the sustainable management of metal contaminated lands. With the assistance of  
4 synchrotron XRF technique, this study investigated possible mechanisms that control the  
5 localization of Fe, Cu, Mn, Pb and Zn in the root tissues of *Typha latifolia* L. collected  
6 from a contaminated wetland. Metal localizations especially in the case of Fe and Pb in  
7 the dermal tissue and the vascular bundles were different. Cluster analysis was performed  
8 to divide the dermal tissue into iron plaque enriched dermal tissue and regular dermal  
9 tissue based on the spatial distribution of Pb and Fe. Factor analysis showed that Cu and  
10 Zn were closely correlated to each other in the dermal tissues. The association of Cu, Zn  
11 and Mn with Fe was strong in both regular dermal tissue and iron plaque enriched dermal  
12 tissue, while significant ( $p < 0.05$ ) correlation of Fe with Pb was only observed in tissues  
13 enriched with iron plaque. In the vascular bundles, Zn, Mn, and Cu showed strong  
14 association, suggesting that the localization of these three elements was controlled by the  
15 similar mechanism. Iron plaque in the peripheral dermal tissues acted as a barrier for Pb  
16 and a buffer for Zn, Cu and Mn. Casparian strip regulated the transportation of metals  
17 from dermal tissues to the vascular bundles. The results suggested that the mechanisms  
18 controlling metal localization in root tissues varied with both tissue types and metals.

1 **Keywords:** Synchrotron  $\mu$ -XRF, Root metal uptake and transportation, Iron plaque,  
2 *Typha latifolia* L., Wetland;

3

#### 4 **1. Introduction**

5 Urban soil contamination has increased dramatically in recent decades due to  
6 anthropogenic activities (Qian *et al.*, 2011; Wuana & Okieimen, 2011; Desouki & Feng,  
7 2012; Luo *et al.*, 2012). Lead (Pb), copper (Cu), manganese (Mn) and zinc (Zn) are  
8 contaminants commonly found in urban soil. Once they enter soil, these metals cannot be  
9 degraded and tend to accumulate in soil and pose potential risks to urban ecological  
10 stability and human health. Urban brownfields are concerned specifically because they  
11 are in densely populated areas and difficult to revitalize (French *et al.*, 2006; Gallagher *et*  
12 *al.*, 2008; Luo *et al.*, 2012). Plants are transplanted in abandoned brownfields to mitigate  
13 soil metal contamination, improve urban ecosystem stability, and remediate soil metal  
14 contamination (McKenna, 1998; French *et al.*, 2006; Dickinson *et al.*, 2009; Desouki &  
15 Feng, 2012;). *Typha latifolia* L. (broadleaf cattail) is a wetland plant that is widely used  
16 for wetland restoration, eutrophic lake clean up, and wastewater effluent treatment (Ye *et*  
17 *al.*, 1997, 1998; Sasmaz *et al.*, 2008; Calheiros *et al.*, 2009). Previous field studies  
18 identified *T. latifolia* L. as a plant species that is capable of tolerating soil with extremely  
19 high metal concentration (McNaughton *et al.*, 1974), which makes it an ideal candidate

1 for metal phytoextraction from the contaminated wetlands to meet remediation purpose  
2 (McNaughton *et al.*, 1974; Ye *et al.*, 1997, 2001; Sasmaz *et al.*, 2008; Brunham &  
3 Bendell, 2010; Grisey *et al.*, 2011; Klink *et al.*, 2012). A better understanding of metal  
4 uptake and translocation processes in the plant will benefit future application of *T.*  
5 *latifolia* L. in environmental management projects.

6           The uptake and translocation of metals by plant root is controlled by many  
7 mechanisms that vary with root tissues. On the surface of wetland plant root, a layer of  
8 amorphous Fe hydroxide named as iron plaque is commonly observed (Ye *et al.*, 1997).  
9 The negative surface charge of iron plaque makes it capable of adsorbing or co-  
10 precipitating metal(loid)s (Ye *et al.*, 1998; Ye *et al.*, 2001). Located at the interface  
11 between soil pore water and root surface dermal tissues, iron plaque plays a role either as  
12 a buffer that enhances metal uptake efficiency, or as a barrier that restricts the  
13 transportation of metals at root surface (Tripathi *et al.*, 2014). On the peripheral part of  
14 the root are dermal tissues, which either uptake metal ions in soil pore water freely  
15 through passive diffusion in the apoplast system, or uptake and transport metals  
16 selectively into the symplast system under the assistance of selective cell membrane  
17 transporters (Taiz & Zeiger, 2010; Marschner, 2012). When metals reach the vascular  
18 bundles in the middle of root, the transportation of substances in the apoplast is blocked  
19 by the Casparian strip and prevents them from entering the vascular bundles. Only metals

1 in the symplastic system can enter the vascular tissue and be further transported to plant  
2 shoot (Brennan & Shelley, 1999; Clemens *et al.*, 2002; Rascio & Navari-Izzo, 2011).  
3 Localization of metals in root tissues indicate possible mechanisms plant root takes to  
4 regulate metal uptake and transportation processes (Marschner, 2012).

5           Recently, the advanced high resolution analytical techniques have provided  
6 micro-scale metal localization information and supported plant metal uptake and  
7 translocation mechanisms studies. For example, Lyubenova *et al.* (2012, 2013) applied  
8 micro-proton induced X-ray emission (micro-PIXE) to analyze the spatial distribution of  
9 18 elements in *T. latifolia* L tissues and observed tissue-specific distribution patterns of  
10 these elements. Synchrotron X-ray absorption near-edge microstructure spectroscopy  
11 (XANES) measurement for identification of Pb and Fe speciation on *T. latifolia* L. roots  
12 surface showed that Pb(II) and Fe(III) are the major species in the iron plaque in the root  
13 epidermis (Feng *et al.*, 2013). In this study, we aimed at investigating the mechanisms  
14 that control the localization of Cu, Fe, Pb, Mn and Zn in *T. latifolia* L. root tissues and  
15 understanding uptake and translocation mechanisms in *T. latifolia* L. root for metal  
16 assimilation.

17

## 18 **2. Methodology**

### 19 2.1. Study Site

1           The study area was chosen in an urban brownfield within Liberty State Park, New  
2 Jersey, with an area of 1 km<sup>2</sup>. This region was once used for railway transportation and  
3 coal storage for a century. As a result of previous industrial activities, high soil metal  
4 concentrations were found in this area (Gallagher *et al.*, 2008; Qian *et al.*, 2012). The  
5 specific site for this study was chosen at a wetland site which is part of a storm water  
6 drainage ditch. Previous studies showed that the total soil metal concentrations of Cu, Pb  
7 and Zn in this wetland were  $124 \pm 51 \mu\text{g g}^{-1}$ ,  $453 \pm 266 \mu\text{g g}^{-1}$  and  $309 \pm 125 \mu\text{g g}^{-1}$ ,  
8 respectively, which were all above the background levels in New Jersey (Cu:  $14 \mu\text{g g}^{-1}$ ,  
9 Pb:  $35 \mu\text{g g}^{-1}$  and Zn:  $22 \mu\text{g g}^{-1}$ ; EPA, 2005) and indicated the site was highly  
10 contaminated (Gallagher *et al.*, 2008).

## 11 2.2. Sample collection and process

12           Because plants in the growing season have the highest metabolism rate and root to  
13 shoot translocation rate, this period is selected to conduct root metal uptake/translocation  
14 mechanism study. The growing season of *T. latifolia* L. usually lasts from May to July in  
15 each year (Tursun *et al.*, 2011). Plant samples were collected from the study site in the  
16 growing season in 2010 and 2011 along the edge of a storm water drainage ditch. After  
17 the collection, the samples were immediately transported to Montclair State University  
18 for laboratory treatment. Bulk soils on the plant roots were removed by hands initially,  
19 then rinsed off soil particles gently with tap water and finally with distilled-deionized

1 water. To prepare the samples for synchrotron XRF analysis, fresh roots were excised  
2 from the plant and then embedded in the Cryo-Embedding compound and then frozen to  
3 a solid at an optimal cutting temperature (OCT) of -20 °C (Feng *et al.*, 2013). The root  
4 sections with 30 µm thickness were then cut from the frozen samples with a cryotome  
5 (Cryostat CM1950, Leica Microsystems) and mounted on a 25 × 76 mm<sup>2</sup> quartz  
6 microscope slide (SPI Supplies®). Two root sections were prepared from one plant  
7 collected in each year. Four root sections were made in total. The prepared root sections  
8 were stored at 4 °C before synchrotron XRF analysis (Zhang *et al.*, 2011).

### 9 2.3. Synchrotron analysis

10         Synchrotron micro X-ray fluorescence (µXRF) analysis on the four root sections  
11 was conducted at X27A Beamline workstation in the National Synchrotron Light Source  
12 at Brookhaven National Laboratory (Upton, NY). The energy range was fixed at 13.5  
13 keV to excite fluoresces of Cu, Fe, Pb, Mn and Zn simultaneously. Optical images of the  
14 root sections were collected with optical microscope before synchrotron XRF analysis.  
15 Before the analysis started, the slide mounted with the samples was oriented at 45° to the  
16 beam and a 13-element Canberra Ge array was used to collect elemental map with a step  
17 size of 10 µm and a dwell time of 7 seconds (Figure 1). The synchrotron XRF data  
18 collection was made at the beamline workstation, and then processed at Montclair State

1 University. NIST Standard Reference Material (SRM) 1832 and 1833 were analyzed  
2 along with the samples during each synchrotron XRF measurement.

3       Longitudinal mapping of metal (Cu Fe, Mn and Zn) distributions in the root  
4 specimens were made at the NSLS X26A beamline using synchrotron  $\mu$ XRF microprobe.  
5 The X-ray energy was set at 13.5 keV. The beam size on the sample was  $7\ \mu\text{m} \times 10\ \mu\text{m}$   
6 with a step size of  $15\ \mu\text{m}$ . The attenuation of the incident X-rays and outgoing X-rays  
7 was relatively low so that the entire thickness of the root was sampled with varying  
8 efficiencies.

## 9 2.4. Root Anatomy

10       Five different types of root tissue could be identified based on optical images of  
11 the root section: epidermis, exodermis, cortex, endodermis, and vascular bundles (Figure  
12 1, a-d).

## 13 2.5. Data processing and analysis

### 14 2.5.1. Tissue data extraction

15       The original micro scale concentration data of metals (Cu, Zn, Mn, Pb and Zn) in  
16 each root section was saved as a matrix and presented as 2D map (Figure 1). Each pixel  
17 in the synchrotron XRF map represents metal concentration in the root section voxel with

1 a resolution of  $10 \times 10 \mu\text{m}^2$  for the 2010 samples, or  $20 \times 20 \mu\text{m}^2$  for the 2011 samples.  
2 Based on root anatomy morphology observed in the optical images, the root dermal  
3 tissues and the vascular bundles (surrounded by endodermis) were identified (Supplement  
4 1) and the data was extracted from the original XRF map using MATLAB (The  
5 MathWorks Inc., version 7.1.0.246). The extracted matrix data were then transformed  
6 into linear form for further statistical analysis.

#### 7 2.5.2. Identification of iron plaque enriched root dermal tissues

8 Many studies have proved that iron plaque exists in peripheral dermal tissues and  
9 it can effectively adsorb metals such as Pb, Mn, Zn and Cu (Greipsson & Crowder, 1992;  
10 St-Cyr & Campbell, 1996; Ye *et al.*, 1997). Iron plaque and regular dermal tissue  
11 accumulate metals through different mechanisms. Therefore, it is critical to separate the  
12 iron plaque enriched dermal tissues from regular dermal tissues in peripheral dermal  
13 tissues before analyzing the relationship between the metals.

14 High sorption of Pb by iron plaque on *Iris pseudacorus* L. root surface has been  
15 already reported (Zhong *et al.*, 2010). Liu *et al.* (2011) also indicate that iron plaque can  
16 increase the sequestration of Pb on *Oryza sativa* L. root surface. The similar spatial  
17 distribution of high concentration of Pb (Figure 1, q, r, s, and t) and Fe (Figure 1, u, v, w,  
18 and x) in *T. latifolia* L. dermal tissues is in consistent with the observation in the above

1 studies that there is strong association between Pb and iron plaque. Therefore, spatial  
2 distributions of Pb and Fe in the dermal tissue were used as an indicator of the existence  
3 of iron plaque in the dermal tissue.

4 Hierarchical cluster analysis was performed based on the spatial distributions of  
5 Pb and Fe in dermal tissues of each sample to investigate the close association between  
6 metal distributions in the dermal tissues and identify dermal tissue region enriched in iron  
7 plaque. The type of joining algorithm used to amalgamate clusters was Ward's method  
8 and the metric for measuring distance between the metals in each case was Euclidean  
9 distance (Burns & Burns, 2008; McDonald, 2009). Root dermal tissues are divided into  
10 two clusters: iron plaque enriched dermal tissues (in short as iron plaque) (CA1) and  
11 regular dermal tissues (CA2) (Figure 2).

### 12 2.5.3. *Data analysis*

13 The metal concentration from synchrotron  $\mu$ XRF measurement was originally in  
14 the units of counts per second (cps). It was then converted to the units of  $\mu\text{g g}^{-1}$  by  
15 calibrating the samples against the NIST SRM 1832 and 1833 thin glass film on  
16 polycarbonate for XRF spectrometry, provided that the root tissue density was  $1.0 \mu\text{g g}^{-1}$ .  
17 This calibration method did not account for differences in sample matrix and assumed  
18 that the absorption correction was not necessary, which works well for thin samples of

1 uniform thickness (Feng *et al.*, 2013, 2015). In statistical analysis, factor analysis was  
2 applied to identify the inherent association between the spatial distribution of Cu, Mn, Fe,  
3 Pb and Zn in both dermal tissues and vascular bundles. Simple linear regression analysis  
4 was performed to explore the relationship between metals. MATLAB (The MathWorks  
5 Inc.), SYSTAT (SYSTAT Software Inc.) and JMP (JMP ®) were applied for statistical  
6 analyses of the data.

7

### 8 **3. Result**

#### 9 3.1. Root anatomy analysis

10 Figure 1 shows the anatomy structure of root sections of *T. latifolia* L. Five  
11 different types of root tissue could be identified, which are epidermis, exodermis, cortex,  
12 endodermis, and vascular bundles (Figure 1). Epidermis, exodermis and the tissue  
13 between are considered as dermal tissues (Figure 1, a-d, ep-ex). Dermal tissue maintains  
14 the selectivity of root uptake from soil by taking up water and nutrients and avoiding  
15 unwanted compounds like toxic substances and soil borne pathogens (Schreiber & Franke,  
16 2011). Cortex tissues include several layers of cells with thin cell walls (Figure 1, a-d, co).  
17 In the middle of the root is vascular bundle, surrounded by a layer of endodermis with the  
18 suberized Casparian strip (Figure 1, a-d, en and va). The vascular bundles selectively

1 transport substances from root cortex tissues and upload the substances to stems and  
2 shoots of the plant (Schreiber & Franke, 2011).

### 3 3.2. Metal localizations in dermal tissues and vascular bundles

4 As indicates by the coefficient of variance for each element in Table 1, metal  
5 localization in root dermal tissues and vascular bundles are highly heterogeneous. Also,  
6 the concentration of one metal element in the same type of tissue from each sample is  
7 different (Figure 1 and Table 1), suggests the accumulation of metals in root is  
8 inconsistent. Nevertheless, the spatial distribution pattern of metals is still very similar  
9 between the four samples (Figure 1, ep-ex)

10 In the dermal tissues, the concentration of Fe is the highest among all the five  
11 elements ranges from  $374 \pm 836 \mu\text{g g}^{-1}$  to  $3709 \pm 4806 \mu\text{g g}^{-1}$  (Table 1, Figure 1). The  
12 coefficient of variance (c.v.) of Zn, Cu and Mn are all less than 1.3, which are much  
13 lower than that of Fe (1.30 – 2.24) and Pb (1.52 – 3.47). These results indicate that  
14 variations in Zn, Cu and Mn distributions in the dermal tissue are less than that of Fe and  
15 Pb (Table 1), they also suggest that the localization of these two groups of element may  
16 be controlled by different mechanisms.

17 In the vascular bundles, the accumulations of the metals are different from that in  
18 the dermal tissue. The average concentration of Zn is the highest, ranging from  $5.87 \pm$

1 5.30  $\mu\text{g g}^{-1}$  to  $964 \pm 666 \mu\text{g g}^{-1}$ , followed by Fe ( $9.82 \pm 5.55 \mu\text{g g}^{-1}$  to  $128 \pm 172 \mu\text{g g}^{-1}$ ),  
2 Mn ( $2.66 \pm 3.95 \mu\text{g g}^{-1}$  to  $50.8 \pm 34.0 \mu\text{g g}^{-1}$ ), Cu ( $4.56 \pm 4.87 \mu\text{g g}^{-1}$  to  $41.8 \pm 15.6 \mu\text{g g}^{-1}$ )  
3 and Pb ( $0.08 \pm 0.41 \mu\text{g g}^{-1}$  to  $6.20 \pm 7.82 \mu\text{g g}^{-1}$ ) (Table 1). In particular, the  
4 concentrations of Fe and Pb in the vascular bundles are almost an order of magnitude  
5 lower than that in the dermal tissue, indicating that these two metals mainly accumulate  
6 in the dermal tissue of the root (Table 1, Figure 1). As shown in Figure 1 (e, f, g, h; i, j, k,  
7 l; m, n, o, p), bright rings of Mn, Cu and Zn are observed around the vascular bundles,  
8 where the Casparian strip is likely located. In a study by Lyubenova *et al.* (2012), the  
9 same bright ring structure was observed in the root sections of *T. latifolia* L. Therefore,  
10 the bright rings of Mn, Cu and Zn around the vascular bundles observed in this study  
11 likely suggest apoplastic transportation and accumulation of Mn, Cu and Zn around the  
12 Casparian strip. Synchrotron  $\mu\text{XRF}$  radiograph images (Figure 3) show the heterogeneity  
13 of metal (Cu, Fe, Mn and Zn) distribution along a 1 cm long root branch. Several “hot  
14 spots” of metals are scattering across the branch. Therefore, heterogeneous distribution of  
15 metals could be observed not only across root sections, but also along the axis of the root.

### 16 3.3. Relationship between the localization of metals in dermal tissues and vascular 17 bundles

18 Since the localization feature of metals is different between the dermal tissues and  
19 the vascular bundles (Figure 1, Table 1), the mechanisms controlling the accumulation of

1 metals in each tissue component should be examined. The association among Pb, Fe, Mn,  
2 Cu, and Zn in their spatial distributions in both dermal tissues and vascular bundles were  
3 analyzed respectively in order to investigate possible mechanisms governing the uptake  
4 and transportation of metals. As shown in Table 1, the coefficients of variance of metal  
5 concentrations in the tissues are greater than 0.5, suggesting a highly heterogeneous  
6 spatial accumulation of metals (Table 1). In order to reduce data skewness disturbs  
7 further statistical analysis, a logarithm ( $\log_{10}$ ) transformation was applied to all the data  
8 (McDonald, 2009). In addition, all the four root samples were collected in the growing  
9 season and they shared the same mechanisms in the regulation of root metal  
10 accumulations (Tursun *et al.*, 2011). Therefore, the spatial distributions of Pb, Fe, Mn, Cu  
11 and Zn from all the four samples were analyzed together. Factor analysis was performed  
12 to explore the internal relationships between the metal spatial accumulation in both  
13 dermal tissues and vascular bundles.

14 In the dermal tissue, three factors with eigenvalue greater than 0.5 are identified,  
15 which explain 92% of the total variance (Table 2). High loadings of Pb (0.95) and Fe  
16 (0.91) are observed in Factor 1 that explains 35.73% of the total variance, indicating  
17 close relationship between Pb and Fe in their spatial distribution in the root dermal tissues.  
18 Sequestration of Pb on wetland plant root surface with iron plaque has been observed in  
19 many studies (e.g., Liu *et al.*, 2007, 2011; Feng *et al.*, 2013). Therefore, Factor 1

1 represents the iron plaque in the dermal tissues. Factor 2, which has high loadings of Cu  
2 (0.95) and Zn (0.93), explains 36.42% of the total variance. This factor indicates a close  
3 association between the distribution of Zn and Cu in the dermal tissue, possibly because  
4 both elements are essential nutrients. Factor 3 accounts for 20.00% of the total variance  
5 with only one high loading element, Mn (0.95).

6 In the vascular bundles, three factors with eigenvalue greater than 0.5 are  
7 identified and explain 90.14% of the total variance (Table 2). Factor 1 explains 47.93%  
8 of the total variance. It has high loadings of Zn (0.92), Mn (0.87) and Cu (0.87), which  
9 are all essential nutrients for plant growth. The other two factors have high loading of  
10 only one specific metal in each factor. Factor 2 has high loading of Pb (0.97) and explains  
11 21.89% of the total variance. Factor 3 has high loading of Fe (0.99) and explains 20.32%  
12 of the total variance (Table 2). The factor analysis suggested that the accumulations of  
13 metals in the dermal tissues and the vascular bundles were controlled by different  
14 mechanisms.

15 In order to investigate the differences in metal localization mechanisms between  
16 the dermal tissues and the vascular bundles, the associations between the spatial  
17 distribution of Cu, Mn, Pb, Fe and Zn in each type of tissue were further investigated.  
18 Simple linear regressions between the localization of metals in each specific type of root  
19 tissue were conducted to explore the association between metals.

1

## 2 **4. Discussion**

### 3 4.1. Effect of iron plaque on the spatial distributions of metals in dermal tissue

4           Because of the high affinity of metal cations to Fe hydroxide, iron plaque plays a  
5 role as either buffer or barrier of metals in the root uptake process. The role of iron  
6 plaque in the uptake of a metal can be judged based on the relationship between Fe and  
7 the metal in the iron plaque. If the correlation between Fe and the metal is strong in the  
8 iron plaque but weak in the regular dermal tissue, then iron plaque eliminates the uptake  
9 of this metal. If the correlation between Fe and the metal was weak in iron plaque but  
10 strong in regular dermal tissue, then iron plaque had no affinity to this metal. If the  
11 correlation between Fe and the metal was strong in both the iron plaque and the regular  
12 dermal tissue, it suggests that the iron plaque has strong affinity to the metal, but does not  
13 eliminate further transportation of the metal. In this case, the iron plaque might be a  
14 buffer of the metal.

15           In this study, a simple linear regression was applied to compare metal localization  
16 patterns (Cu, Mn, Pb and Zn) between iron plaque and regular dermal tissues (Figure 4).  
17 According to Figure 4, Pb has significant ( $p < 0.05$ ) positive correlation with Fe in the iron  
18 plaque in all the four root samples (Figure 4, A, B, C and D) with  $r^2 > 0.5$ , suggesting a

1 significant correlation between Fe and Pb in the iron plaque. However, the association  
2 between Fe and Pb in regular dermal tissues is rather weak (Figure 4). As shown in Table  
3 3, the concentration of Pb is rather low in the inner rim of the dermal tissue. In addition,  
4 extremely low accumulation of Pb is observed in the cortex tissues and the vascular  
5 bundles in this study (Table 1, Figure 1), indicating that very limited amount of Pb was  
6 transported to the rest part of the plant tissues. Very likely, iron plaque acts as a barrier  
7 for the uptake of Pb in *T. latifolia* L.

8           Similar to Pb, the correlations between Fe and three essential elements (Mn, Zn,  
9 and Cu) are significant ( $p < 0.05$ ) in the iron plaque, indicating that iron plaque can co-  
10 precipitate these metals (Figure 4). In the regular dermal tissues, however, the  
11 correlations of Mn, Zn and Cu with Fe are inconsistent. Both significant (Figure 4, E, F,  
12 H, I, J, L, M, and P) and insignificant (Figure 4, G, K, N and O) correlations are observed.  
13 The results suggest that Fe and the three other metals (Mn, Zn and Cu) may not share the  
14 same transport and accumulation mechanisms in the regular dermal tissues.

15           The effect of iron plaque on the localization of Cu, Mn and Zn in the root  
16 peripheral dermal tissue was further investigated by comparing the correlation among the  
17 three elements in the iron plaque and the regular dermal tissues (Figure 5). Generally  
18 speaking, although the concentrations of Mn, Zn and Cu are higher in the iron plaque,  
19 there is no obvious difference in the associations between the three elements in the iron

1 plaque and the regular dermal tissues (Figure 5). The association of metals with cell wall  
2 is determined by the concentration of metal cations in soil solution and the competition  
3 between metal cations (Schreiber & Franke, 2011). As shown in Figure 5, the association  
4 between essential metals (Mn, Fe and Cu) is similar no matter whether it is in iron plaque  
5 or in the regular dermal tissues, suggesting that the accumulations of these metals is  
6 possibly controlled by the same mechanism. The only difference is that iron plaque  
7 adsorbs more Mn, Zn and Cu, causing high accumulation of these metals within the Fe  
8 plaque. These observations are in consistent with previous studies conducted by St-Cyr &  
9 Campbell (1996) and Batty *et al.* (2000) who suggested that the adsorption and co-  
10 precipitation of Cu, Mn and Zn with iron plaque should not influence the further root  
11 uptake of these metals. Therefore, iron plaque possibly acts as a buffer for the  
12 accumulation of Mn, Zn and Cu in *T. latifolia* L.

#### 13 4.2. Spatial distributions of metals in vascular bundles

14 Vascular bundles bridge the exchange of nutrients between roots and shoots and  
15 upload mineral nutrients from roots to shoots through xylem. In this study, high  
16 concentrations of Zn, Mn and Cu on the Casparian strip around the vascular bundles were  
17 observed (Figure 1). Similar rings with high metal concentrations around the endodermis  
18 were also observed by Yamaguchi *et al.* (2011). They exposed *Solanum torvum* (Cd  
19 excluder) and *Sloanum melongena* (Cd accumulator) to high concentration of Cd and

1 found Cd concentration around the endodermis was higher in *Solanum torvum* than that  
2 in *Solanum melongena* (Yamaguchi *et al.*, 2011). Therefore, it is possible that the  
3 Casparian strip in the root may delay the transportation of Zn, Mn and Cu from apoplast  
4 to symplast.

5 In order to examine the similarity or difference in metal (Zn, Mn and Cu)  
6 accumulation mechanisms between the dermal tissues and the vascular bundles, the  
7 correlations between Zn and Mn, Zn and Cu, and Mn and Cu in both types of tissue were  
8 compared (Figure 6). Significant ( $p < 0.05$ ) positive correlations were observed between  
9 Mn and Zn, indicating the similar uptake and transport mechanisms between these two  
10 elements. In previous studies it was found that Zn and Mn could be taken up by *T.*  
11 *latifolia* L. from the rhizosphere soil more effectively than Cu (Sasmaz *et al.*, 2008; Klink  
12 *et al.*, 2012), and Mn and Zn usually shared the same transporters, such as ZIP and  
13 IRT1 in the root tissue (Hall & Williams, 2003).

14 The slopes of the regression lines for metal correlations show nearly no difference  
15 between the dermal tissues and the vascular bundles in most cases (Figure 6). Different  
16 trends in the regression lines between the two types of tissues are only observed in a few  
17 cases (Figure 6 D, H, and L). In addition, no distinct boundaries between the scatter plots  
18 from the two tissues are observed (Figure 6). Therefore, the similar relationship of Zn, Cu,

1 and Mn between the dermal tissue and the vascular bundles indicate that these three  
2 elements accumulated in the two types of tissues possibly follow the same mechanism.

### 3 **5. Conclusion**

4 This study investigated the spatial distributions of Fe, Cu, Mn, Pb and Zn in *T.*  
5 *latifolia* L. roots during the growing season to explore possible mechanisms that govern  
6 metal localizations in root tissues. In the peripheral dermal tissues, the accumulations of  
7 metals in the roots were highly spatially heterogeneous and varied with the root tissue  
8 types and the metals themselves. There were significant correlations between the spatial  
9 distribution of Pb and Fe in the iron plaque enriched dermal tissues. At the same time, the  
10 correlations between Cu and Zn were significant in both iron plaque enriched dermal  
11 tissue and regular dermal tissues. Moreover, concentrations of Cu and Zn were higher in  
12 the iron plaque enriched dermal tissues, which suggests that iron plaque possibly acts as a  
13 barrier of Pb and a buffer of Zn and Cu in metal transport in dermal tissues. In the  
14 vascular bundles, significant correlations were observed between the spatial localization  
15 of Zn, Mn and Cu, especially between Mn and Zn, indicating the three metals may share  
16 similar localization mechanisms in the vascular bundles. Finally, the close association  
17 trends between the spatial distribution of Zn, Mn and Cu in the dermal tissues and the  
18 vascular bundles suggest that these two types of tissues may accumulate the three  
19 elements in a similar mechanism. This study demonstrates that synchrotron XRF

1 technique can provide an innovative approach to study metal assimilation in the plants  
2 and explore the mechanism of plant metal uptake and transportation. The results can be  
3 used as a reference to advise biological modification of metal uptake and translocation  
4 rate of *T. latifolia* L. from a micro scale perspective.

5

## 6 **Acknowledgements**

7 This work was supported in part by the China Scholarship Council (YQ) and the  
8 Margaret and Herman Sokol Foundation (HF). This project was also supported in part by  
9 the U.S. Department of Energy, Office of Science, Office of Workforce Development for  
10 Teachers and Scientists (WDTS) under the Visiting Faculty Program (VFP) (HF). Use of  
11 the NSLS was supported by the U.S. Department of Energy, Office of Science, Office of  
12 Basic Energy Sciences, under Contract No. DE-AC02-98CH10886. NSLS X27A was  
13 supported in part by the U.S. Department of Energy - Geosciences (DE-FG02-  
14 92ER14244 to The University of Chicago - CARS). We are also grateful to Dr. Steve  
15 Heald, Co-Editor of Journal of Synchrotron Radiation, and two anonymous reviewers  
16 who offered constructive comments and suggestions on an earlier draft of this paper.

17

1

2 **6. References**

3 Batty, L. C., Baker, A. J. M., Wheeler, B. D. & Curtis, C. D. (2000). *Annals of Botany* **86**,

4 647-653.

5 Brennan, Mark A. & Shelley, M. L. (1999). *Ecological Engineering* **12**, 271-297.

6 Brunham, W. & Bendell, L. I. (2010). *Water, Air, & Soil Pollution* **219**, 417-428.

7 Burns, R. & Burns, R. (2008). *Business Research Methods and Statistics Using SPSS*.

8 London: SAGE Publications Ltd.

9 Calheiros, C. S., Rangel, A. O. & Castro, P. M. (2009). *Bioresource Technology* **100**,

10 3205-3213.

11 Clemens, S., Palmgren, M. G. & Kramer, U. (2002). *Trends in Plant Science* **7**, 309-315.

12 Desouki, S. H. & Feng, H. (2012). *Metal Contamination Sources, Detection and*

13 *Environmental Impact*, edited by H. Shao, pp. 81-94. New York: NOVA Science

14 Publishers, Inc.

15 Dickinson, N. M., Baker, A. J. M., Doronila, A., Laidlaw, S. & Reeves, R. D. (2009).

16 *International Journal of Phytoremediation* **11**, 97-114.

- 1 Feng, H., Qian, Y., Gallagher, F. J., Wu, M., Zhang, W., Yu, L., Zhu, Q., Zhang, K., Liu,  
2 C. J. & Tappero, R. (2013). *Environmental Science and Pollution Research International*  
3 **20**, 3743-3750.
- 4 Feng, H., Qian, Y., Gallagher, F., Zhang, W., Yu, L., Liu, C.-J., Jones, K.W. & Tappero,  
5 R. (2015). *Journal of Environmental Science*, accepted.
- 6 French, C. J., Dickinson, N. M. & Putwain, P. D. (2006). *Environmental Pollution* **141**,  
7 387-395.
- 8 Gallagher, F. J., Pechmann, I., Bogden, J. D., Grabosky, J. & Weis, P. (2008).  
9 *Environmental Pollution* **153**, 351-361.
- 10 Greipsson, S. & Crowder, A. (1992). *Canadian Journal of Botany* **70**, 824-830.
- 11 Grisey, E., Laffray, X., Contoz, O., Cavalli, E., Mudry, J. & Aleya, L. (2011). *Water, Air,*  
12 *& Soil Pollution* **223**, 1723-1741.
- 13 Hall, J. L. & Williams, L. E. (2003). *Journal of Experimental Botany* **54**, 2601-2613.
- 14 Klink, A., Macioł, A., Wisłocka, M. & Krawczyk, J. (2012). *Limnologica - Ecology and*  
15 *Management of Inland Waters* **43**, 164-168.
- 16 Liu, H. J., Zhang, J. L. & Zhang, F. S. (2007). *Environmental and Experimental Botany*  
17 **59**, 314-320.

- 1 Liu, J., Leng, X., Wang, M., Zhu, Z. & Dai, Q. (2011). *Ecotoxicology and Environmental*  
2 *Safety* **74**, 1304-1309.
- 3 Luo, X. S., Yu, S., Zhu, Y. G. & Li, X. D. (2012). *The Science of the Total Environment*  
4 **421-422**, 17-30.
- 5 Lyubenova, L., Pongrac, P., Vogel-Mikus, K., Mezek, G. K., Vavpetic, P., Grlj, N.,  
6 Kump, P., Necemer, M., Regvar, M., Pelicon, P. & Schroder, P. (2012). *Metallomics* **4**,  
7 333-341.
- 8 Lyubenova, L., Pongrac, P., Vogel-Mikus, K., Mezek, G. K., Vavpetic, P., Grlj, N.,  
9 Regvar, M., Pelicon, P. & Schroder, P. (2013). *Journal of Hazardous Materials* **248-249**,  
10 371-378.
- 11 Marschner, P. (2012). *Marschner's Mineral Nutrition of Higher Plants*, 3rd ed. USA:  
12 Academic Press.
- 13 McDonald, J. H. (2009). *Handbook of Biological Statistics*. Sparky House Publishing  
14 Baltimore, MD.
- 15 McKenna, G. F. (1998). *Risk-Based Corrective Action and Brownfields Restorations*,  
16 edited by Benson, C.H., Meegoda, J.N., Gilbert, R.B., & Clemence, S.P., pp16-29,  
17 Geotechnical Special Publication.

- 1 McNaughton, S. J., Folsom, T. C., Lee, T., Park, F., Price, C., Roeder, D., Schmitz, J. &  
2 Stockwell, C. (1974). *Ecology* **55**, 1163-1165.
- 3 Merchant, S. S. (2010). *Plant Physiology* **154**, 512-515.
- 4 Qian, Y., Feng, H., Zhang, W., Yu, L., Zhu, Q., Zhang, L. & Wang, X. (2011). *Heavy*  
5 *Metal Sediments*, edited by L. H. Sanz, pp. 59-85: NOVA Publishers, Inc.
- 6 Qian, Y., Gallagher, F. J., Feng, H. & Wu, M. (2012). *Environmental Pollution* **166**, 23-  
7 30.
- 8 Rascio, N. & Navari-Izzo, F. (2011). *Plant Science* **180** 169-181.
- 9 Sasmaz, A., Obek, E. & Hasar, H. (2008). *Ecological Engineering* **33**, 278-284.
- 10 Schreiber, L. & Franke, R. B. (2011). *eLS*, JohnWiley & Sons, Ltd,  
11 doi:10.1002/9780470015902.a0002086.pub2.
- 12 St-Cyr, L. & Campbell, P. G. (1996). *Biogeochemistry* **33**, 45-76.
- 13 Taiz, L. & Zeiger, E. (2010). *Plant Physiology*, Sinauer Associates, Inc.
- 14 Tripathi, R. D., Tripathi, P., Dwivedi, S., Kumar, A., Mishra, A., Chauhan, P. S., Norton,  
15 G. J. & Nautiyal, C. S. (2014). *Metallomics* **6**, 1789-1800.

- 1 Tursun, N., Seyithanoglu, M., Uygur, F. N., Elibuyuk, I. O. & Elibuyuk, E. A. (2011).  
2 *Flora - Morphology, Distribution, Functional Ecology of Plants* **206**, 731-735.
- 3 Wuana, R. A. & Okieimen, F. E. (2011). *ISRN Ecology* **2011**, 1-20.
- 4 Yamaguchi, N., Mori, S., Baba, K., Kaburagi-Yada, S., Arao, T., Kitajima, N., Hokura, A.  
5 & Terada, Y. (2011). *Environmental and Experimental Botany* **71**, 198-206.
- 6 Ye, Z. H., Baker, A. J. M., Wong, M. H. & Willis, A. J. (1997). *The New Phytologist* **136**,  
7 469-480.
- 8 Ye, Z. H., Baker, A. J. M., Wong, M. H. & Willis, A. J. (1998). *Aquatic Botany* **61**, 55-67.
- 9 Ye, Z. H., Cheung, K. C. & Wong, M. H. (2001). *Canadian Journal of Botany* **79**, 314-  
10 320.
- 11 Zhang, J., Tian, S., Lu, L., Shohag, M.J., Liao, H., Yang, X. (2011). *Journal of*  
12 *Hazardous Materials* **197**, 264-271.
- 13 Zhong, S., Shi, J. & Xu, J. (2010). *Journal of Soils and Sediments* **10**, 964-970.
- 14



Table 1 Metal concentrations (Mean  $\pm$  S.D.) ( $\mu\text{g g}^{-1}$ ) and ranges (Min-Median-Max) ( $\mu\text{g g}^{-1}$ ) of Cu, Fe, Mn, Pb and Zn in the root sections collected in the tip and middle of *T. latifolia* L. collected in 2010 and 2011.

Sample	Element	n	Dermal Tissues				C.V.	Vascular Bundles					
			Min	Max	Median	Mean		n	Min	Max	Median	Mean	C.V.
			$\mu\text{g g}^{-1}$	$\mu\text{g g}^{-1}$	$\mu\text{g g}^{-1}$	$\mu\text{g g}^{-1}$		$\mu\text{g g}^{-1}$	$\mu\text{g g}^{-1}$	$\mu\text{g g}^{-1}$	$\mu\text{g g}^{-1}$		
2010 (I)	Fe*	531	BDL	33464	2373	3709	1.30	836	BDL	1661	30.7	88.0	1.87
	Cu		BDL	76.0	16.9	18.7	0.59		BDL	41.8	9.46	11.1	0.74
	Zn*		19.7	666	179	188	0.54		BDL	453	73.7	104	0.78
	Mn*		BDL	240	50.5	56.9	0.70		BDL	138	15.9	25.7	1.07
	Pb*		BDL	916	38.2	62.2	1.65		BDL	30.6	BDL	2.22	2.05
2010 (II)	Fe*	659	n.d.	14667	328	862	1.82	541	BDL	772	59.0	75.9	1.08
	Cu*		3.68	212	41.5	44.2	0.47		BDL	96.2	40.3	41.8	0.37
	Zn*		29.6	1466	468	510	0.51		BDL	4027	742	964	0.69
	Mn*		1.33	203	28.0	29.6	0.55		BDL	199	38.9	50.8	0.67
	Pb*		BDL	422	3.01	9.63	2.86		BDL	11.4	BDL	0.61	2.21
2011 (I)	Fe*	532	65.80	13821	349	1710	1.48	235	55.8	1786	95.7	128	1.35
	Cu		BDL	43.3	3.17	4.45	1.17		BDL	28.8	3.54	4.56	1.07
	Zn		BDL	188	25.2	35.0	0.91		0.77	192	31.6	38.3	0.84
	Mn*		BDL	113	22.2	27.0	0.71		BDL	85.6	17.9	20.8	0.64
	Pb*		BDL	468	16.1	54.4	1.52		BDL	33.5	2.36	6.20	1.26
2011 (II)	Fe*	880	BDL	9022	71.9	374	2.24	293	BDL	26.3	10.2	9.82	0.57
	Cu*		BDL	60.9	8.41	10.0	0.84		BDL	17.1	5.56	5.55	0.65
	Zn*		BDL	252	14.2	23.7	1.26		BDL	27.5	5.14	5.87	0.90
	Mn*		BDL	259	8.89	22.4	1.52		BDL	22.7	BDL	2.66	1.49
	Pb*		BDL	70.0	BDL	1.86	3.47		BDL	3.51	BDL	0.08	5.05

\* Significant difference between metal accumulation in the dermal tissue and the vascular bundle (Wilcoxon test,  $p < 0.05$ ).

Table 2 Results of factor analysis based on localization of Cu, Fe, Mn, Pb and Zn in the dermal tissue and vascular bundle (Rotated loading matrix, Varimax rotation, Gamma = 1.000).

Dermal tissues				Vascular bundles			
Parameter	Factor 1	Factor 2	Factor 3	Parameter	Factor 1	Factor 2	Factor 3
$\log_{10}(\text{Fe})$	<b>0.95</b>	-0.07	0.13	$\log_{10}(\text{Zn})$	<b>0.92</b>	-0.24	0.06
$\log_{10}(\text{Pb})$	<b>0.91</b>	0.17	0.22	$\log_{10}(\text{Mn})$	<b>0.88</b>	0.20	0.14
$\log_{10}(\text{Cu})$	0.01	<b>0.95</b>	0.09	$\log_{10}(\text{Cu})$	<b>0.87</b>	-0.22	-0.01
$\log_{10}(\text{Zn})$	0.08	<b>0.93</b>	0.14	$\log_{10}(\text{Pb})$	-0.12	<b>0.97</b>	0.15
$\log_{10}(\text{Mn})$	0.25	0.18	<b>0.95</b>	$\log_{10}(\text{Fe})$	0.09	0.14	<b>0.99</b>
Percent of total variance explained	35.7	36.4	20.0	Percent of total variance explained	47.9	21.9	20.3

Table 3 Accumulation ( $\mu\text{g g}^{-1}$ ) of Fe in the iron plaque and regular dermal tissues from *T. latifolia* L. root sections collected in 2010 and 2011.

Sample	Iron plaque					Regular dermal tissues				
	n	Min $\mu\text{g g}^{-1}$	Max $\mu\text{g g}^{-1}$	Median $\mu\text{g g}^{-1}$	Mean $\pm$ S.D. $\mu\text{g g}^{-1}$	n	Min $\mu\text{g g}^{-1}$	Max $\mu\text{g g}^{-1}$	Median $\mu\text{g g}^{-1}$	Mean $\pm$ S.D. $\mu\text{g g}^{-1}$
2010 (I)	404	187.00	33464	3720	4845 $\pm$ 4996	127	BDL	406	78.2	92.7 $\pm$ 73
2010 (II)	320	BDL	14667	810	1499 $\pm$ 2035	336	BDL	3765	158.0	261.0 $\pm$ 377
2011 (I)	250	439.00	13820	2517	3446 $\pm$ 2814	282	65.8	632	144.0	170 $\pm$ 87
2011 (II)	202	394.00	9021	856.0	1351 $\pm$ 1334	678	BDL	387.0	36.0	82.30 $\pm$ 95.6

Figure captions:

Figure 1 Optical images and concentration ( $\mu\text{g g}^{-1}$ ) spatial distribution of Cu, Mn, Pb, Fe and Zn in *T. latifolia* L. root sections in the tip and the middle of roots collected in 2010 and 2011. ep: epidermis; ex: exodermis; co: cortex; en: endodermis ca: Casparian strip; va: vascular tissues (a-d, optical images of root tissue sections; e-h, spatial distribution of Zn; i-l, spatial distribution of Cu; m-p, spatial distribution of Mn; q-t, spatial distribution of Pb; u-x, spatial distribution of Fe).

Figure 2 Iron plaque region and regular dermal tissue region identified by the cluster analysis in the dermal tissues of four root sections (A-D, CA1 iron plaque region; E-H, CA2 regular dermal tissue). The concentration scale bar indicated the concentration of Fe in the XRF map, the regions traced by white line indicate identified clusters.

Figure 3 Spatial accumulation of Cu, Fe, Mn and Zn in whole root collected in *T. latifolia* L. collected in 2010.

Figure 2 Simple linear regressions between  $\log_{10}(\text{Fe})$  and the other four metals  $\log_{10}(\text{Pb})$ ,  $\log_{10}(\text{Cu})$ ,  $\log_{10}(\text{Zn})$  and  $\log_{10}(\text{Mn})$  in the iron plaque region and regular dermal tissue region of the dermal tissues in the root sections collected in 2010 and 2011 (open circle  $\circ$ : iron plaque region; solid circle  $\bullet$ : regular dermal tissue. A, E, I, M: root section collected from root (I) of 2010 *T. latifolia* L.; B, F, J, N: root section collected from the (II) of 2010 *T. latifolia* L.; C, G, K, O: root section collected from the (I) of 2011 *T. latifolia* L.; D, H, L, P: root section collected from the (II) of 2011 *T. latifolia* L.).

Figure 3 Simple linear regressions between essential nutrients  $\log_{10}(\text{Cu})$ ,  $\log_{10}(\text{Zn})$  and  $\log_{10}(\text{Mn})$  in the iron plaque region and regular dermal tissue region of the dermal tissues in the root sections collected in 2010 and 2011 (open circle  $\circ$ : iron plaque region; solid circle  $\bullet$ : regular dermal tissue. A, E, I: root section collected from root (I) of 2010 *T. latifolia* L.; B, F, J: root section collected from (II) of 2010; C, G, K: root section collected from the (I) of 2011 *T. latifolia* L.; D, H, L: root section collected from the (II) of 2011 *T. latifolia* L.).

Figure 4 Simple linear regressions between essential nutrients  $\log_{10}(\text{Cu})$ ,  $\log_{10}(\text{Zn})$  and  $\log_{10}(\text{Mn})$  in the dermal tissues and vascular bundles of the root sections collected in 2010 and 2011 (open circle  $\circ$ : dermal tissues; solid circle  $\bullet$ : vascular bundles. A, E, I: root section collected from root (I) of 2010 *T. latifolia* L.; B, F, J: root section collected from (II) of 2010; C, G, K: root section collected from the (I) of 2011 *T. latifolia* L.; D, H, I: root section collected from the (II) of 2011 *T. latifolia* L.).

Supplemental Material 1: root tissue groups separation based on the optical images of root samples from the four root section samples. Green: dermal tissues; Blue: Endodermis surrounded vascular bundles.

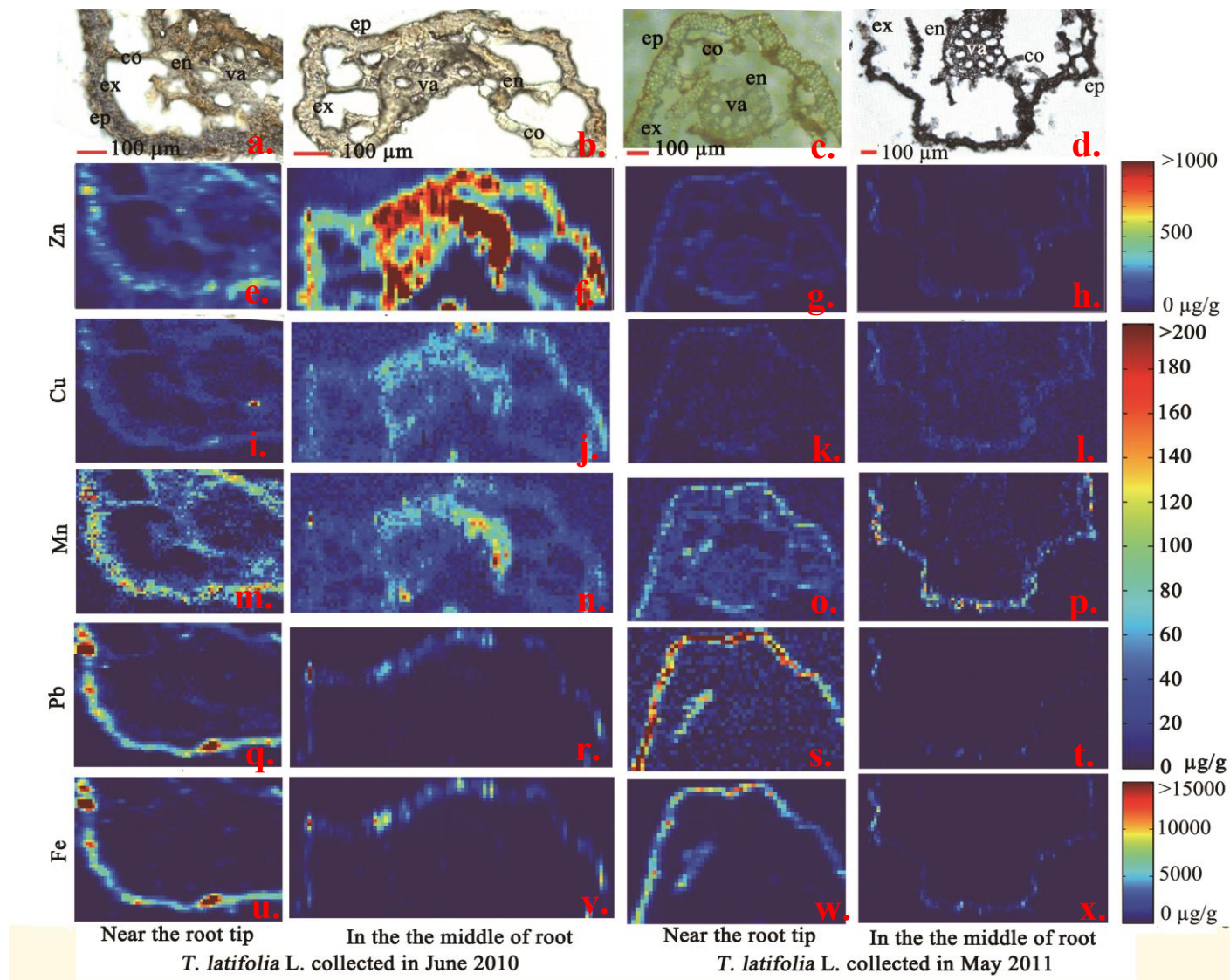
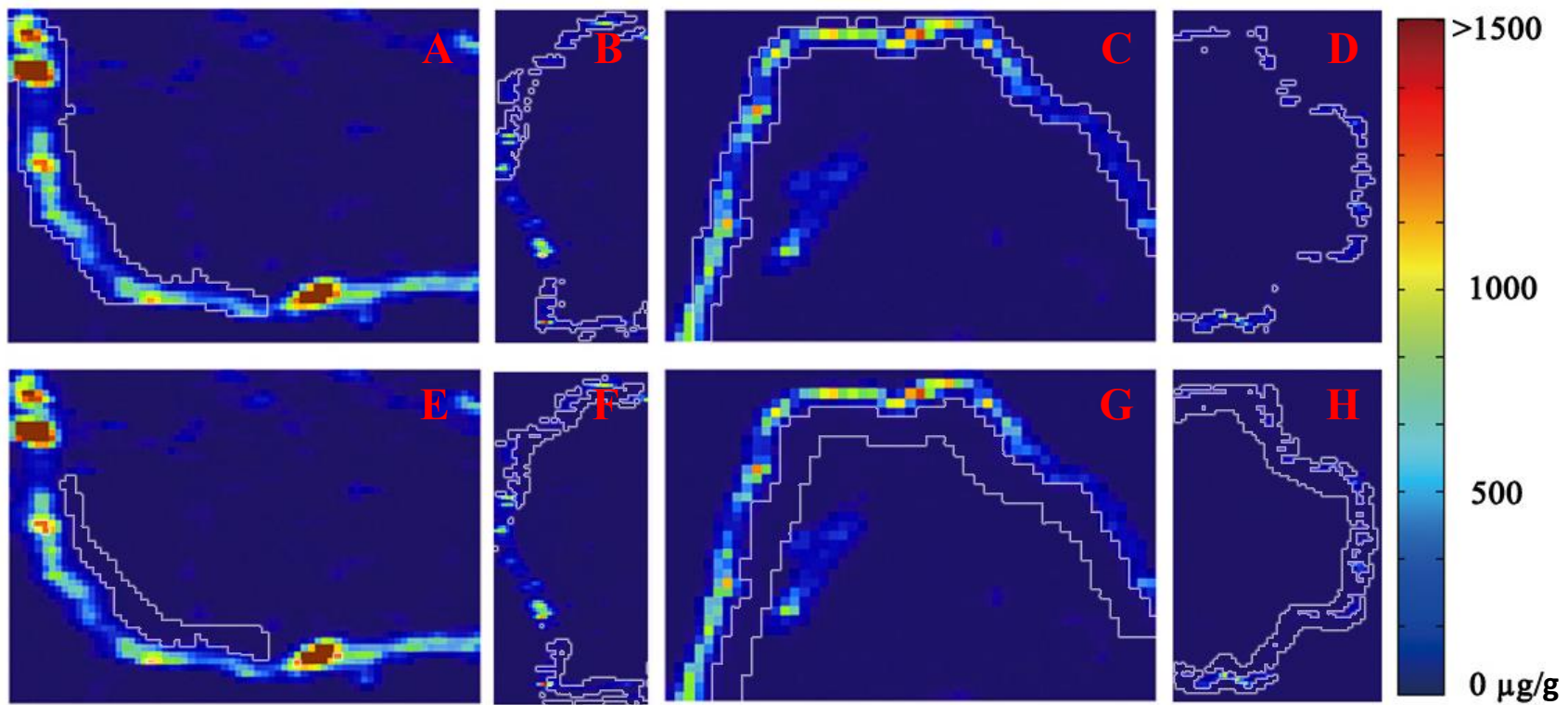


Figure 1: Optical images and concentration ( $\mu\text{g g}^{-1}$ ) spatial distribution of Cu, Mn, Pb, Fe and Zn in *T. latifolia* L. root sections in the tip and the middle of roots collected in June 2010 and May 2011. ep: epidermis; ex: exodermis; co: cortex; en: endodermis ca: Casparian strip; va: vascular tissues (a-d, optical images of root tissue sections; e-h, spatial distribution of Zn; i-l, spatial distribution of Cu; m-p, spatial distribution of Mn; q-t, spatial distribution of Pb; u-x, spatial distribution of Fe).



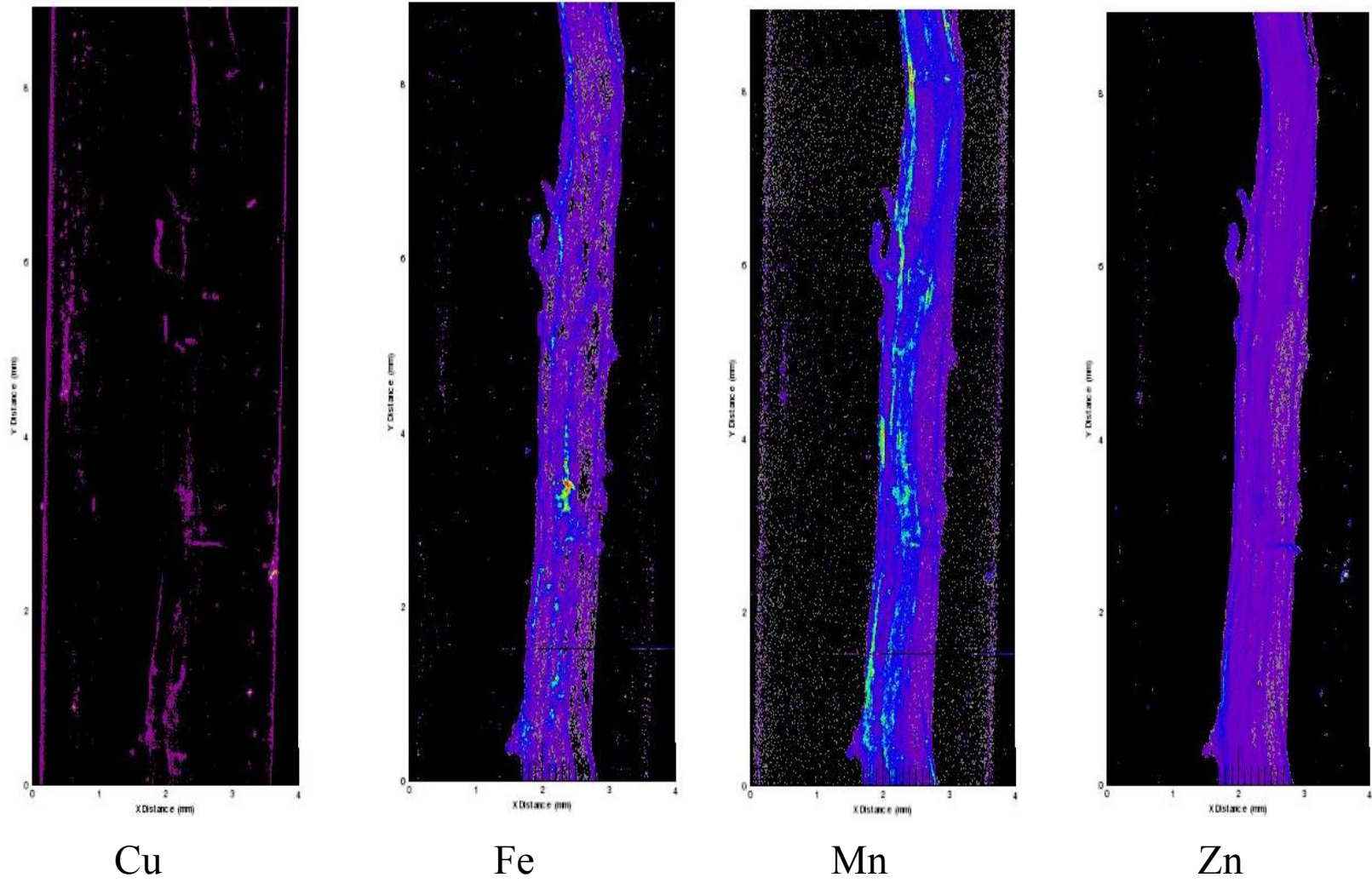
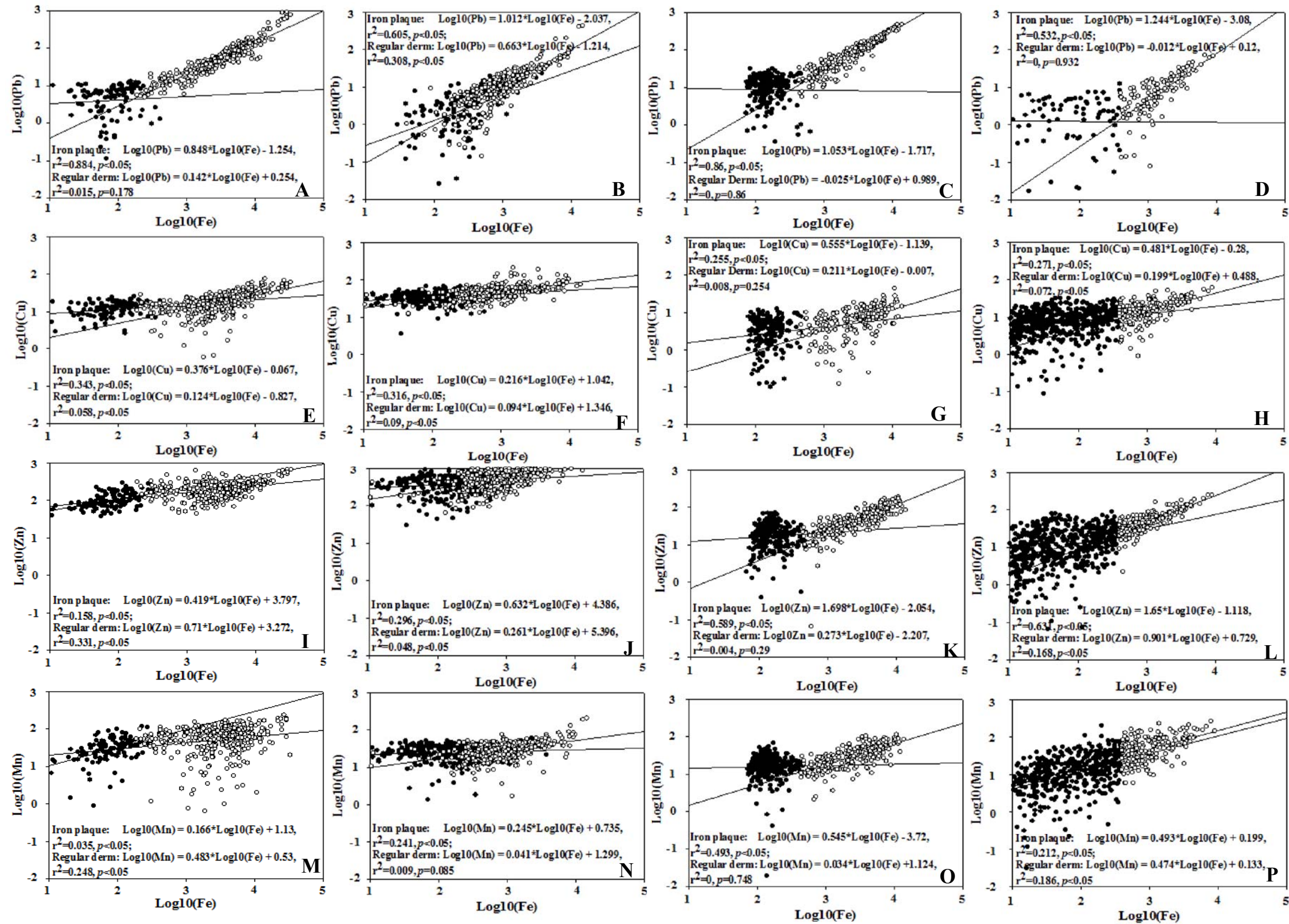
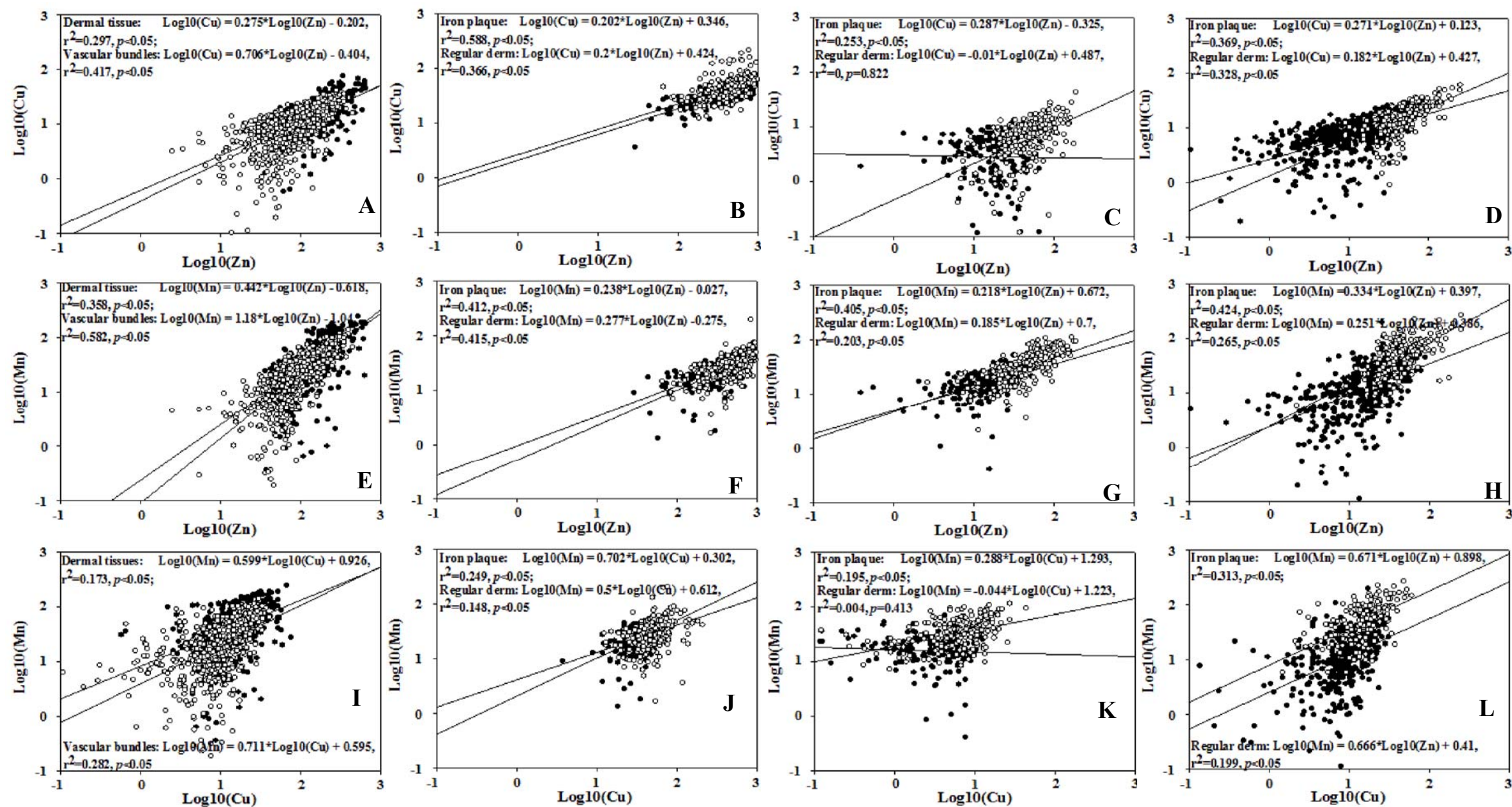


Figure 2. Spatial accumulation of Cu, Fe, Mn and Zn in whole root collected in *T. latifolia* L. collected in June 2010.



**Figure 4.** Simple linear regressions between  $\text{Log}_{10}(\text{Fe})$  and the other four metals  $\text{Log}_{10}(\text{Pb})$ ,  $\text{Log}_{10}(\text{Cu})$ ,  $\text{Log}_{10}(\text{Zn})$  and  $\text{Log}_{10}(\text{Mn})$  in the iron plaque region and regular dermal tissue region of the dermal tissues in the root sections collected in June 2010 and May 2011. (open circle  $\circ$ : iron plaque region; solid circle  $\bullet$ : regular dermal tissue. A, E, I, M: root section collected from root tip of June 2010 *T. latifolia* L.; B, F, J, N: root section collected from the middle of June 2010 *T. latifolia* L.; C, G, K, O: root section collected from the tip of May 2011 *T. latifolia* L.; D, H, L, P: root section collected from the middle of May 2011 *T. latifolia* L.)



**Figure 5.** Simple linear regressions between essential nutrients Log<sub>10</sub>(Cu), Log<sub>10</sub>(Zn) and Log<sub>10</sub>(Mn) in the iron plaque region and regular dermal tissue region of the dermal tissues in the root sections collected in June 2010 and May 2011. (open circle ○: iron plaque region; solid circle ●: regular dermal tissue. A, E, I: root section collected from root tip of June 2010 *T. latifolia* L.; B, F, J: root section collected from root middle of June 2010; C, G, K: root section collected from the tip of May 2011 *T. latifolia* L.; D, H, L: root section collected from the middle of May 2011 *T. latifolia* L.)

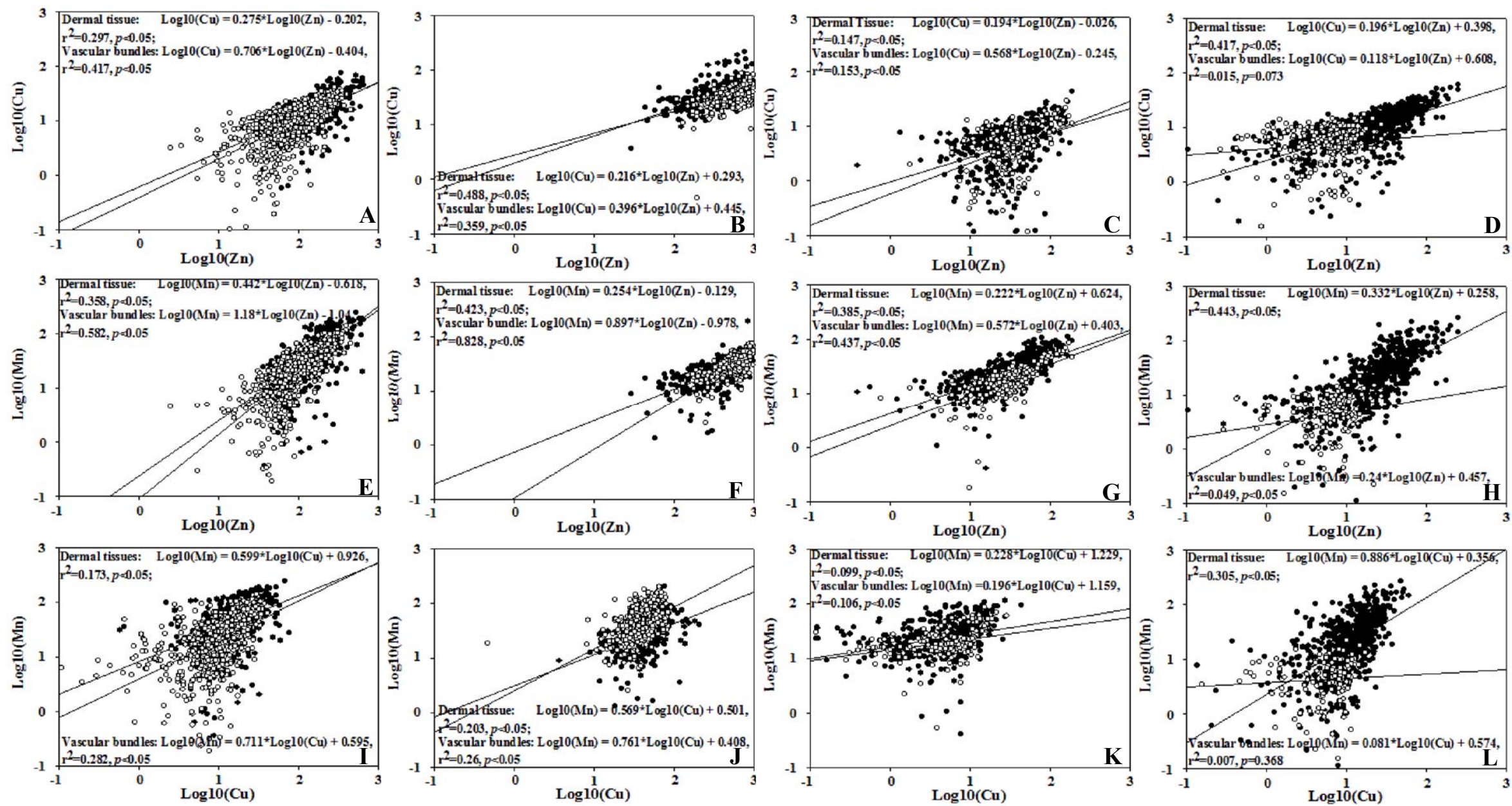


**Figure 6.** Simple linear regressions between essential nutrients Log<sub>10</sub>(Cu), Log<sub>10</sub>(Zn) and Log<sub>10</sub>(Mn) in the dermal tissues and vascular bundles of the root sections collected in June 2010 and May 2011. (open circle ○: dermal tissues; solid circle ●: vascular bundles. A, E, I: root section collected from root tip of June 2010 *T. latifolia* L.; B, F, J: root section collected from root middle of June 2010; C, G, K: root section collected from the tip of May 2011 *T. latifolia* L.; D, H, L: root section collected from the middle of May 2011 *T. latifolia* L.)

